LINEAR MOTION CARRIAGE WITH BEARINGS PRELOADED BY INCLINED IRON CORE LINEAR ELECTRIC MOTOR

Alexander Slocum[1], Murat Basaran, Roger Cortesi
Massachusetts Institute of Technology
77 Massachusetts Avenue, Room 3-445
Cambridge, MA, 02139 USA
slocum@mit.edu Fax 603.224.5369 phone 603.253.0012

Abstract

A fundamentally precise and simple linear motion axis design is presented where the attractive force from the linear motor is used to preload an air-bearing supported carriage that moves on two intersecting perpendicular planes. These two planes represent the most accurate and lowest cost geometry that can be created to guide linear motion. By placing the motor at a desired position and angle with respect to the air bearing pads, desired preload forces can be obtained on the pads. Because the attractive forces are typically 5 times the axial force generated by the motor, the system is inherently well preloaded and stable even in the presence of large externally applied forces that might induce pitch, yaw, or roll.

1. Introduction

Linear motion axes are ubiquitous in manufacturing systems, where for high speed or high accuracy systems, rolling element bearings or pressurized fluid bearings are most often used. To reduce cost and increase simplicity, open-face iron-core linear motors are desirable for high-speed systems, but they can cause excessive loading and premature failure of rolling element bearings. Fig. 1 illustrates a new design for a fundamentally precise and simple linear motion axis where the attractive force from the linear motor is used to preload an air-bearing supported carriage where the air bearings ride on two intersecting perpendicular planes. These two planes represent the most accurate and the lowest cost geometry that can be created to guide linear motion. By placing the motor at a desired position and angle with respect to the air bearing pads, any desired distribution of preload force can be obtained on the pads. Because the attractive forces are typically 5 times the axial force from the motor, the system is inherently well preloaded and stable even in the presence of large externally applied forces that might induce pitch, yaw, or roll. This concept can also be used with angular motion axes, particularly where partial rotary motion is required as shown in Fig. 2.

[1] Corresponding author. All authors can be reached at this address

The advantage of this type of design is that a system built from such components could be rapidly assembled from modular components.

2. Background

A key element of any fluid film bearing is that large areas and small gaps create the opportunity for large damping by squeeze films. Squeeze film damping is inversely proportional to the cube of the bearing gap. On the other hand, bearing stiffness is inversely proportional to the gap; hence combined with the mass of the system, dynamic performance can vary widely, and it is impractical to generalize on what is the optimal bearing gap. Indeed, it has been proposed that machine performance can be optimized in real time by dynamically controlling the bearing pad position and/or the bearing gap. For example, spindle designs have also been tested that use piezoelectric actuators to radially adjust the position of fluidstatic bearing pads supported by flexures [1] which in effect controls spindle error motion and also can affect the bearing gap. With this design, dynamic radial motion of a spindle at 1000 rpm can be reduced by a factor of 2. Liquid bearings do not suffer from pneumatic hammer caused by excessive volume downstream of the restrictor, and this has allowed for the control of the pressure in the bearing pocket using a servo valve [2], but this leads to increased cost and complexity. A compromise is a diaphragm type restrictor, where the inlet flow resistance is made proportional to flow using a diaphragm [3].

Devitt of New Way Bearings[2] has been using a hybrid approach, where he lets his porous carbon bearings actually physically contact the rail surface, while providing enough air pressure to overcome most of the static force the bearings must support. In this way, the effect of the gap is essentially eliminated, but the system does require a very high mechanical impedance actuator, such as a ballscrew, to overcome the static friction that is present.

Bearing supply pressure affects the gap, and hence the system damping which in turn can affect the process for which the machine is used. As will be discussed in the results section, if the supply pressure is too high, then chatter can occur in a grinding application. It is likely therefore that as this machine design evolves, supply pressure could be controlled in a quasi-static fashion by the machine tool controller changing the supply pressure in anticipation of the use of a known process. Accelerometers could also be used to sense the onset of chatter and adjust the supply pressure accordingly. In either case, this will cause a

[2] Unpublished work, New Way builds and sells such systems, and the results appear promising. See http://www.newwaybearings.com

change in bearing gap, which would cause a change in tool offset; hence this would require the controller to incorporate either real time measurement of the gap (expensive) or the use of a look-up table to compensate.

3. Design Method

Porous graphite bearings are selected because they are very damage resistant. Porous carbon air bearing performance can be predicted [5], but for commercially available bearings, design data (bearing gap as a function of area, pressure, and force) is typically directly obtained from the manufacturer as shown in Fig. 3. Table 1 shows data taken from Fig. 3 and analyzed to give the observed stiffness efficiency h: stiffness = h *Area*P_{supply}/gap, and to determine the damping parameters as described below. The bearings have an "optimal" design region where the gap (lift) is 6 to 15 microns. When the supply pressure is increased, the stiffness decreases because the gap increases for a given load, and the damping ζ also decrease.

The squeeze film damping b (N/m/s) for a rectangular bearing with width w, and length L, gap h, and fluid viscosity μ can be estimated from [6] to be:

$$K_S = 0.7925 - \frac{1.1005}{e^{w/L}} + \frac{0.0216}{w/L} + 0.0153\, w/L \tag{1.1}$$

$$b = K_s \frac{m w^3 L}{h_o^3} \tag{1.2}$$

For a second order model of a carriage supported by air bearings, with a total mass m of the carriage and attached components, and total bearing stiffness k, the second order system damping factor z can be determined:

$$\begin{aligned} &m\ddot{x} + b\dot{x} + kx = 0 \\ &\ddot{x} + 2V\omega_n\dot{x} + \omega_n^2 x = 0 \\ &V = \frac{b}{2\sqrt{km}} \end{aligned} \tag{1.3}$$

If z is greater than 0.7, then the system will be very well damped and not likely to chatter. This is the source of the misnomer that a system can have too much stiffness; on the contrary, a system can have too little damping. In the case of a magnet preloaded bearing system, if the supply pressure is increased in the belief that this should give greater stiffness, as is the case for the bearings preloaded by geometric constraints, the stiffness will actually decrease

because the gap increases. The squeeze film damping coefficient is a function of the gap cubed, and hence damping will drop significantly. This is illustrated in Fig. 4.

In order to obtain the desired effect of preloading the bearings evenly using the linear electric motor's permanent magnets, a simple force balance can be used as shown in Fig. 5. For each of the forces, there are associated x, y, z coordinates that bear similar subscripts. For the bearings *i*, the coordinates of their centers of stiffness are x_i, y_i, and z_i. There are six unknown bearing forces and the unknown motor actuation force. The preload force F_{mm} provided by the magnets is assumed constant. These 7 unknowns can be solved for using force and moment balance about all three axes and a constraint equation requiring bearings 2, 3, 5, and 6 to remain in a plane even as they deflect. Assuming bearing linear stiffness $\delta_i = F_{Bi}/k_i$, the following equilibrium equations result:

$$[A] = \begin{bmatrix} -1 & 0 & 0 & -1 & 0 & 0 & 0 \\ 0 & 1 & 1 & 0 & 1 & 1 & 0 \\ 0 & 0 & 0 & 0 & 0 & 0 & 1 \\ 0 & z_2 & z_3 & 0 & z_5 & z_6 & -y_m \\ z_1 & 0 & 0 & z_4 & 0 & 0 & x_m \\ -y_1 & -x_2 & -x_3 & -y_4 & -x_5 & -x_6 & 0 \\ 0 & \dfrac{1}{k_2(x_2 - x_3)} & \dfrac{-1}{k_3(x_2 - x_3)} & 0 & \dfrac{-1}{k_5(x_5 - x_6)} & \dfrac{1}{k_6(x_5 - x_6)} & 0 \end{bmatrix} \tag{1.4}$$

$$[B] = \begin{bmatrix} F_{mm}\sin q + F_{Px} \\ -F_{mm}\cos q - m_c g - m_s g + F_{Py} \\ -m_c a - m_s a + F_{Pz} \\ -F_{mm} z_m \cos q - m_c g z_c - m_s g z_s + F_{Py} z_p - F_{Pz} y_p \\ -F_{mm} z_m \sin q - F_{Px} z_p + F_{Pz} x_p \\ -F_{mm} x_m \cos q + F_{mm} y_m \sin q + m_s g x_s + m_c g x_c + F_{Px} y_p - F_{Py} x_p \\ 0 \end{bmatrix} \tag{1.5}$$

$$\begin{bmatrix} F_{B1} & F_{B2} & F_{B3} & F_{B4} & F_{B5} & F_{B6} & F_m \end{bmatrix}^T = -[A]^{-1}[B] \tag{1.6}$$

These equations are easily solved using an Excel™ spreadsheet, which also makes it convenient for inputting the design parameters, as shown in Fig. 6[3]. Here it was assumed that the bearing stiffness was equal to the product of the bearing area and supply pressure divided by one-half the nominal bearing gap. Note that to very accurately predict machine performance, a full detailed error budget should be performed [7], or ideally a study of the probabilities of combinations of errors and their net effect on work volume accuracy [8].

[3] This spreadsheet is also used for the estimated system dynamics calculations of Fig. 4 and for analyzing bearing data in Table 1. It is available from http://pergatory.mit.edu/research/axtrusion

Fig. 7 shows the outputs, where the spreadsheet's *solver* function can be used to vary parameters to minimize error motions at the tool point. The effect of varying magnet preload force could also be studied, as well as the effect on system dynamic performance.

4. Experimental Systems

To verify the ease of construction and assembly hypothesis, simple prototypes using machined steel rails with carriages supported by cam followers and preloaded by permanent magnets. The simple prototypes for linear and angular motion systems are shown in Fig. 8. These simple "sketch models" verified the robustness of the design and the ease with which the systems could be manufactured.

The next step was to build a precision bench level experiment system to evaluate the manufacturing process and to determine the effect of the motor's iron core passing over the permanent magnets. The bearing rails were made from granite to ensure that the bearings would not be damaged should they slide across the rails after something might have been dropped on them; and it was easier to obtain finished granite components. In anticipation of high speed application, and to increase the ease with which the carriages could be moved around the lab, the carriages were cast from magnesium. For a precision machine tool, however, this would mean even tighter temperature control would have to be maintained.

The bearings were installed by holding them to the granite rail surfaces using vacuum, and then the carriage was placed over them and held so its precision surfaces were parallel to the rail using fixtures as shown in Fig.s 9 and 10, and the proper motor gap is set with a shim. Epoxy was then injected in the region between the backs of the bearings and pockets within the carriage [9]. After the bearings are potted in place with epoxy, the air is turned on and the carriage rises, and the shim can be removed. The original thought was to make modular "L" shaped elements that could then be bolted together to form a machining center.

4.1 Bench level Experiment Results

The pitch was measured as shown in Fig. 11, was found to be a respectable +/- 1 arc-second, with a repeatability on the order of ¼ arc-second. For high precision systems, two motor coils or additional iron could be spaced apart to balance forces and reduce pitching moments. The straightness (moving straightedge) was measured and the results shown in Fig. 12, and showed that in the center, where there is no pitch component, the straightness is on the order of 0.3 μm, which is the tolerance of the granite surfaces.

Experimental modal analysis was conducted on the system to obfuscate concerns that magnet preloaded air bearings, i.e., a carriage not supported by “wrap around” preloaded bearings, may not be well-damped enough for machining applications. Table 2 shows typical results, commensurate with the types of damping values predicted in Table 1. The stiffness of the carriage, as measured at points 2, 3, 4, and 5 was evaluated by placing a weight at the center of the carriage and then measuring the deflection at the points indicated in Fig. 13. The values were respectively 6149, 250, 556, and 235 N/μm. It is strange that the forward part of the carriage appears stiffer than the rear, because it is fully symmetric. The air lines were checked and it did not appear that there was any restriction, and it is unlikely that the bearings themselves have significantly different porosity; thus when the next system is constructed the bearings will be evaluated individually prior to installation.

5. Manufacture and Testing of the Bench Level Prototype Grinder

The goal of the Bench Level Prototype Grinder, shown in Fig. 14, was to determine of the linear motor driven axes could be servo controlled to produce coordinated motion suitable for grinding. In order to set up the servos, the two identical axes, from the bench Level Experiments, were placed on an available wooden workbench so their actuators, encoders, and spindles could be connected to the servo amplifiers and the PC-based Machine tool controller.

PC-Control was from MachineMate™, model number MM1. Encoders were Heidenhain LS403 and Renishaw RGH22, both with A&B quadrature output (5V TTL). Motors were Anorad LCK-2 open faced linear motors, connected to Ultra 3000™ Allen-Bradley servo amplifiers. Current and velocity loops were closed within the servos, while the position was closed using the PC-Control. The system integrated with the electronics was actually ready long before a base was to become available; hence it was decided to go ahead and rough ID grind some sample parts shown in Fig. 15. The results for this quickly assembled system, as shown in Table 3, are actually quite reasonable and thus justified the next step, which is the design of a beta prototype production grinder.

The part was clamped by a collet chuck, which was ground in place to minimize the run-out and provide the best clamping condition. The work spindle was driven by belt drive motor at 600 rpm (approx. 0.8 m/s surface speed) and the grinding spindle had a resin bonded vitrified grinding wheel (20 mm diameter and the length was equal to the part length) the spindle was also belt driven at 30,000 rpm (40 m/s surface speed). The grinding process was done by using a "dress before finish" and oscillating grinding method (approx 8Hz)

during rough and finish grinding. Rough grinding was done with a fast feed rate (0.005mm) until 0.050 mm stock left to the finish size , then the grinding wheel was dressed with a single point diamond and started for finish grinding the remaining stock. At the end of the finish grind the grinding wheel was allowed to spark out by 6 seconds. The coolant was a 5:1 water/oil mixture and the pressure was 2 bar.

The process was very smooth and quiet which meant the wheel was cutting free and the feed rate could be increased for more aggressive grinding. However, the clamping system was not strong enough and the part became loose when the feed rate increased. Therefore, it was not possible to optimize the grinding cycle to minimize cycle time. However, the machine was stiff enough to grind a chatter-free part and remove stock better than a similarly sized and equipped production machine. It should be noted that as anticipated when the bearing supply pressure was increased by several bar, chatter was encountered; hence there is an optimal bearing supply pressure which causes the bearing gap to form to achieve an appropriate level of damping.

6. Conclusions

The design performed as predicted and its manufacturing simplicity means that an axis can virtually be extruded (hence the name "Axtrusion" [10]). Accordingly, designs have since evolved for a simple aluminum extrusion whose bearings surfaces have been flycut and anodized as is common practice in the manufacture of CMMs. Future work will focus on modeling the pitch error as a function of motor coil/magnet interaction, and strategies will be developed to minimize this error further. The spreadsheet can be downloaded from http://pergatory.mit.edu/axtrusion

Acknowledgements

The authors would like to thank Andrew Devitt of New Way Bearings Inc. for supplying the porous carbon air bearings and for assistance in installing them; Anorad Corporation for their generous donation of the linear motor for the first test system; Gerry Parrot of Rock of Ages Corporation for manufacturing the granite; and Phil Greene of Dover Instrument Corporation for helping us integrate the a controller with the motor and to perform the metrology experiments. Finally, Overbeck Machine Tool of Long Island NY provided the resources for creating and testing the bench level prototype; and Jeff Roblee and Fred Mispel of Precitech Inc. of Keene NH measured the parts that were ground on the bench level prototype.

References

[1] Horikawa O., et al.. Vibration, Position, and Stiffness Control of an Air Journal Bearing. 1989 Int. Precis. Eng. Symp., Monterey CA, pp. 321-332.

[2] Zeleny J. Servostatic Guideways-A New Kind of Hydraulically Operating Guideways for Machine Tools. Proc. 10th Int. Mach. Tool Des. Res. Conf., Sept. 1969. Also see U.S. Patents 4,630,942 and 4,080,009.

[3] Degast, J. U.S. Patent 3,442,560, May 6, 1969.

[4] Rowe W. Hydrostatic and Hybrid Bearing Design, Butterworth, London, 1983.

[5] Rasnick WH, et al.. Porous Graphite Air-Bearing Components as Applied to Machine Tools. SME Tech. Report MRR74-02

[6] Fuller DD. Theory and Practice of Lubrication for Engineers; 2nd edition. John Wiley & Sons, New York, 1984.

[7] Slocum AH. Precision Machine Design. Prentice Hall, Eaglewood Cliffs, New Jersey 1992.

[8] Frey DD, Otto KN, and Pflager W. Swept envelopes of cutting tools in integrated machine and workpiece error budgeting. 1997 Annals of the CIRP, vol. 46, no. 1, pp. 475-480.

[9] Devitt A, Slocum A. Method for Manufacturing Externally Pressurized Bearing Assemblies. US Patent 5,488,771, Feb. 6, 1996.

[10] Slocum AH. Linear motion carriage system and method with bearings preloaded by inclined linear motor with high attractive force. US Patent 6,150,740, Nov., 2000.

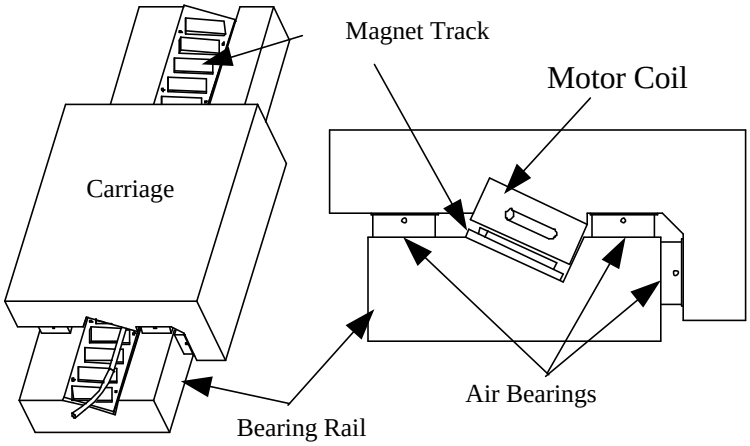

Fig. 1 "Axtrusion" linear motion axis concept where an iron-core open-face linear electric motor's permanent magnets are used to preload aerostatic bearings

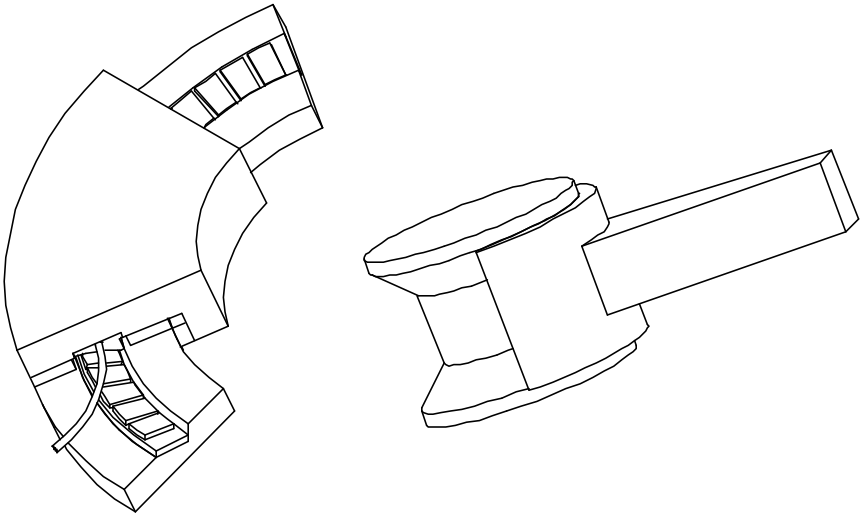

Fig. 2 "Axtrusion" angular motion axis design concepts where fundamentally the rotor is an arc segment: (L) an iron-core open-face rotary electric motor's permanent magnets are located on a conical surface and used to preload aerostatic bearings; (R) conical bearings with magnets that would be on a cylindrical surface

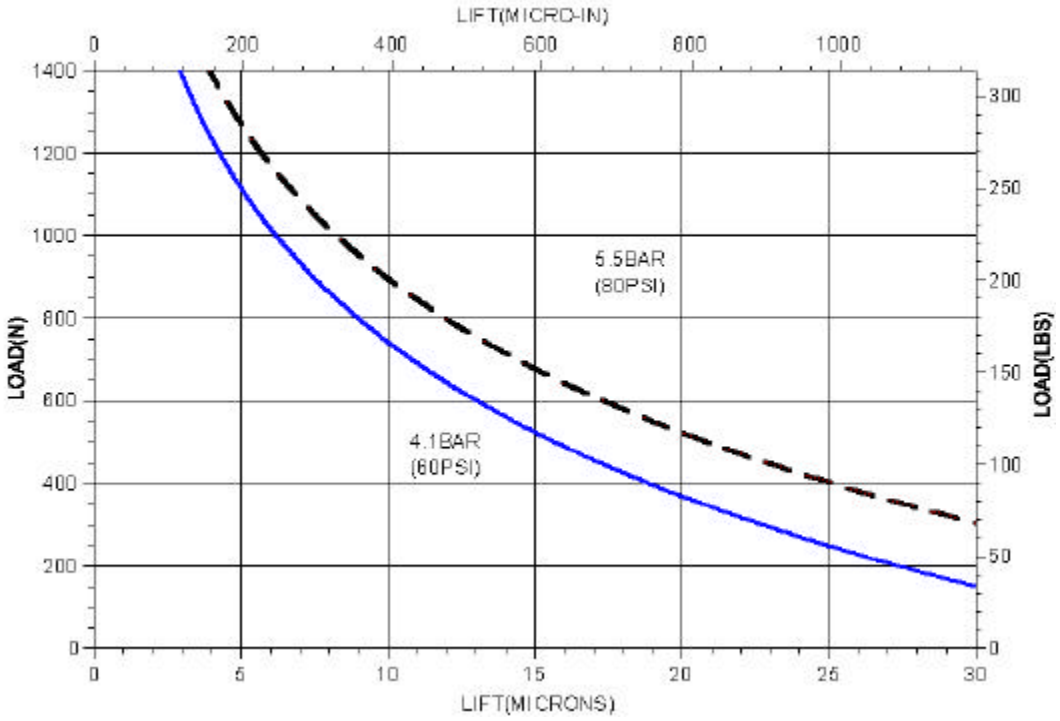

Fig. 3 Load versus gap height and pressure for 50mm x 100 mm commercially available porous graphite air bearing pad (www.newwaybearings.com)

Estimated System Dynamics (squeeze film damping)		
Supply pressure (N/mm^2)	**0.35**	**0.55**
Bearing width, w (mm)	**50**	
Bearing length, L (mm)	**100**	
Air viscosity, mu (N-s/m^2)	**1.40E-05**	
gap (mm)	**0.015**	**0.024**
Ks	**0.176**	
damping, b (N/(m/s)	**9117**	**2349**
Total mass, m (kg)	**130**	
Total stiffness, k (N/mm)	**116667**	**47245**
damping factor, zeta	**0.04**	**0.01**
Percent damping	**7%**	**3%**
Quality (dynamic amplification) factor Q	**13.5**	**33.4**

Fig. 4 Estimated effects of supply pressure on system performance, showing more is often not better for force-preloaded air bearings

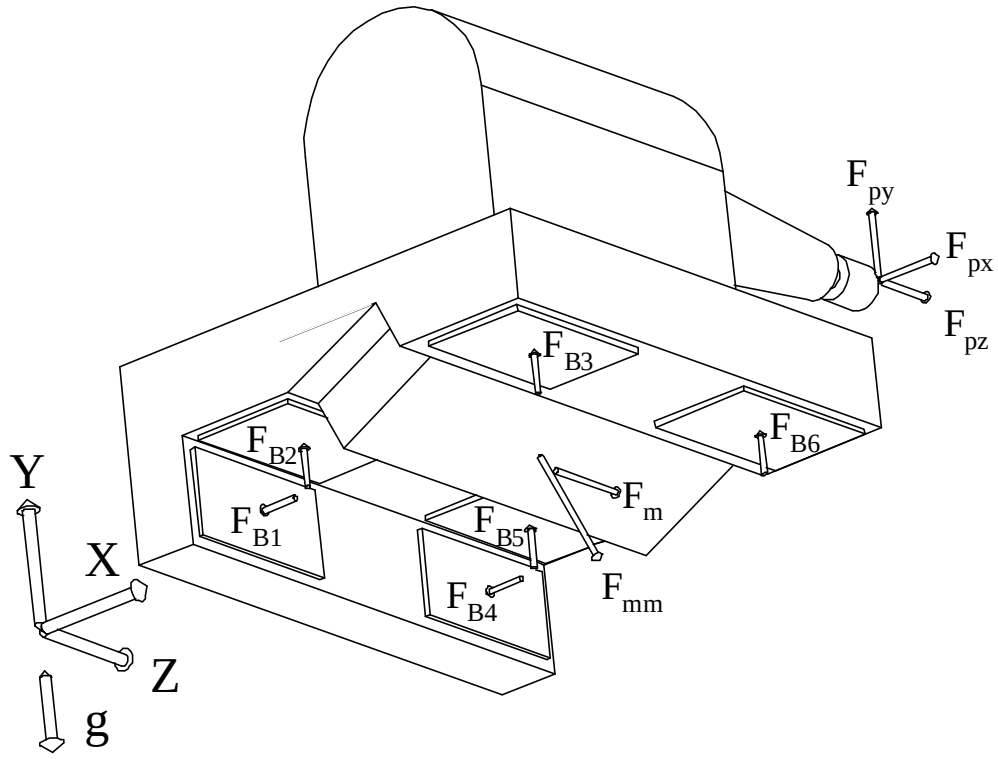

Fig. 5 Generalized forces on the carriage; Note that the mass of the carriage and its location (m_c, x_c, y_c, z_c) and the spindle (m_s, x_s, y_s, z_s) are not shown

Inputs (N, mm) in BOLD, Outpus in RED					
Ps (N/mm^2, psi)	**0.35**	**51**	Bearing supply pressure		
gap, h (mm)	**0.015**		Nominal bearing gap		
a (m/s^2, g)	**0.1**	**0.98**	Axis acceleration		
gravity, g	**9.8**				
bearing efficiency, eta	**0.25**				
Bearing 1		**Bearing 2**		**Bearing 3**	
A_1 (mm^2)	**15000**	A_2	**5000**	A_3	**5000**
K_1 (N/mm)	**87500**	K_2	**29166.667**	K_3	**29166.667**
X_1	**50**	X_2	**100**	X_3	**250**
Y_1	**100**	Y_2	**175**	Y_3	**175**
z_1	**-150**	z_2	**-150**	z_3	**-150**
Bearing 4		**Bearing 5**		**Bearing 6**	
A_4	**15000**	A_5	**5000**	A_6	**5000**
K_4	**87500**	K_5	**29166.667**	K_6	**29166.667**
X_4	**50**	X_5	**100**	X_6	**250**
Y_4	**100**	Y_5	**175**	Y_6	**175**
z_4	**150**	z_5	**150**	z_6	**150**
Process		**Spindle**		**Carriage**	
Fpx (N)	**20**	Mass ms (kg)	**100**	Mass mc (kg)	**30**
Fpy (N)	**20**	Xs	**250**	Xc	**175**
Fpz (N)	**2**	Ys	**300**	Yc	**200**
Xp	**150**	Zs	**50**	Zc	**0**
Yp	**300**	**Motor**			
Zp	**225**	Magnet preload Fmm (N)		**500**	
		Kservo (N/mm)		**500000**	
		Xm		**150**	
		Ym		**150**	
		Zm		**0**	
		theta (rad, deg)		**0.524**	**30**

Fig. 6 Axtrusion design spreadsheet input parameters

Deflections at Process Point (microns, microradians)				
	Process only	Mass, Accel.	Angular	
δx	1.229	12.91	Pitch (ε_x)	0.002
δy	0.703	-13.96	Yaw (ε_y)	-0.001
δz	-0.31	3.47	Roll (ε_Z)	-0.007

Results of Bearing Force and Deflection analysis											
All Loads				Preload only				Process Forces only			
Forces (N)		Defl. (microns)		Forces (N)		Defl. (microns)		Forces (N)		Defl. (microns)	
FB1	184	δ1	-2.10	FB1	125	δ1	-1.43	FB1	-5	δ1	0.06
FB2	50	δ2	-1.70	FB2	103	δ2	-3.52	FB2	-13	δ2	0.45
FB3	581	δ3	-19.91	FB3	114	δ3	-3.90	FB3	17	δ3	-0.58
FB4	86	δ4	-0.99	FB4	125	δ4	-1.43	FB4	25	δ4	-0.29
FB5	263	δ5	-9.01	FB5	103	δ5	-3.52	FB5	-27	δ5	0.93
FB6	794	δ6	-27.22	FB6	114	δ6	-3.90	FB6	3	δ6	-0.10
Fm	125	δservo	-0.25	Fm	0	δservo	0.00	Fm	-2	δservo	0.00

Location of Pitch, Yaw, Roll Axis					
Pitch Axis		Yaw Axis		Roll Axis	
		Xya	50	Xra	175
Ypa	175			Yra	175
Zpa	0	Zya	0		

Deflections (microns, microradians) at approximate center of stiffness											
Mass, Acceleration, Process				Preload Only				Process Only			
δx	0.11	Pitch (ε_x)	-0.024	δx	1.429	Pitch (ε_x)	0.000	δx	0.114	Pitch (ε_x)	0.002
δy	-10.75	Yaw (ε_y)	0.004	δy	-3.712	Yaw (ε_y)	0.000	δy	0.171	Yaw (ε_y)	-0.001
δz	-0.25	Roll (ε_Z)	-0.119	δz	0.00	Roll (ε_Z)	-0.003	δz	0.00	Roll (ε_Z)	-0.007

Fig. 7 Axtrusion design spreadsheet outputs

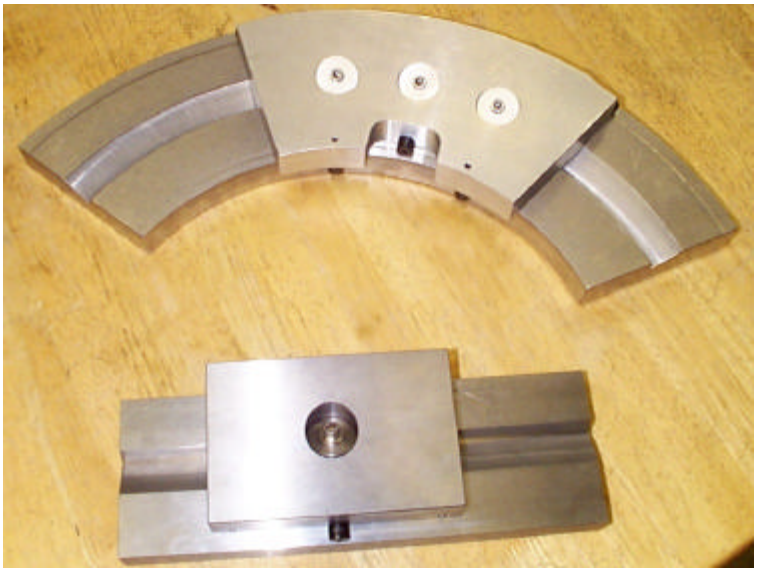

Fig. 8 Proof-of-concept models for linear and angular motion Axtrusions

Fig. 9 Prototype components prior to assembly

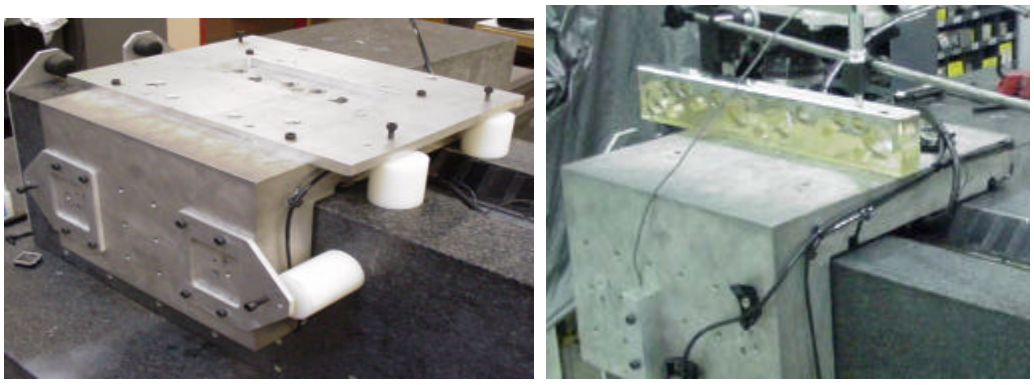

Fig. 10 Prototype system with bearings being replicated in-place, and during metrology tests

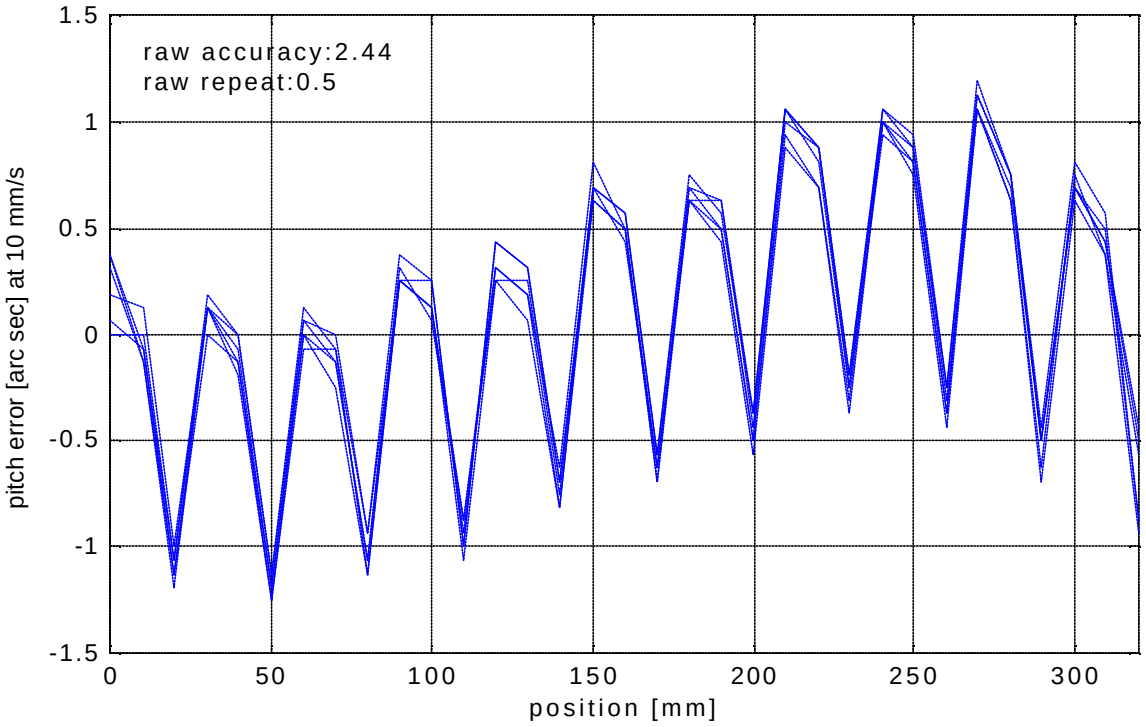

Fig. 11 Pitch motion of the carriage; the period is equal to the magnet pitch

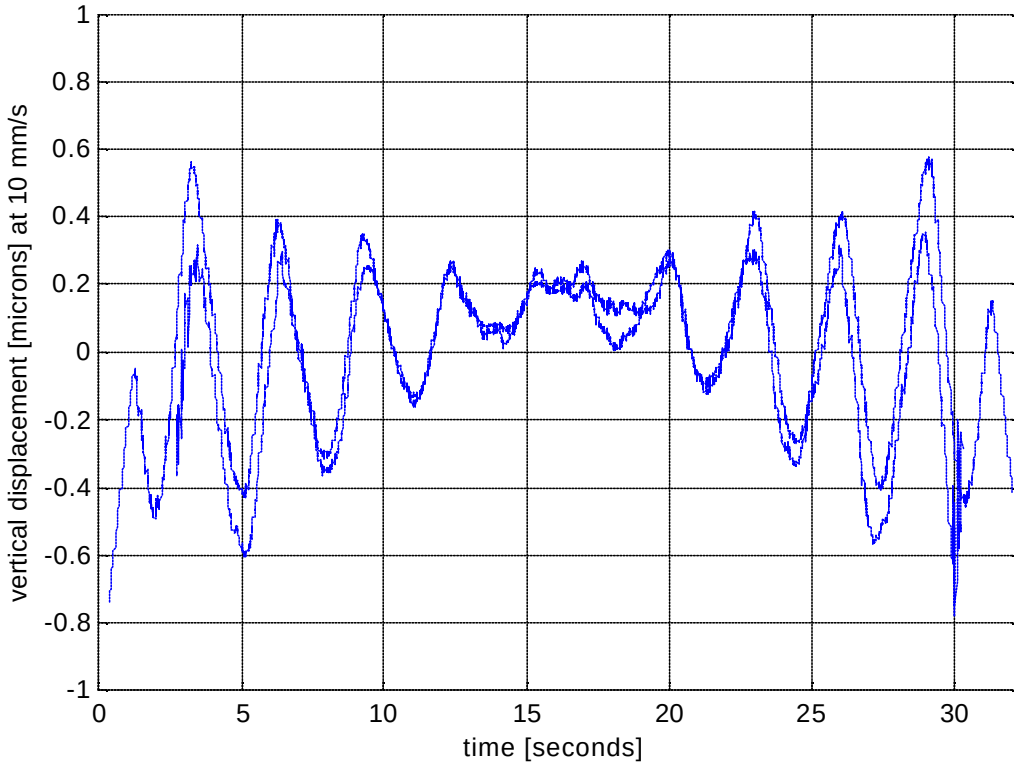

Fig. 12 Straightness measurements (moving straightedge as shown in Fig. 10)

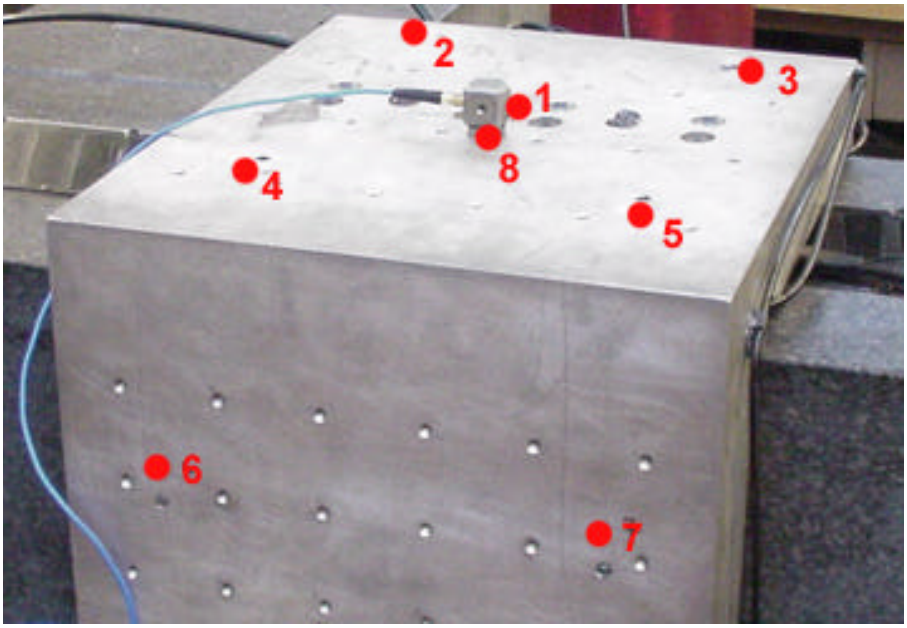

Fig. 13 The carriage and the 8 points used fo r modal analysis. Point 1 is the impact point, and Points 2-7 are the measurement points.

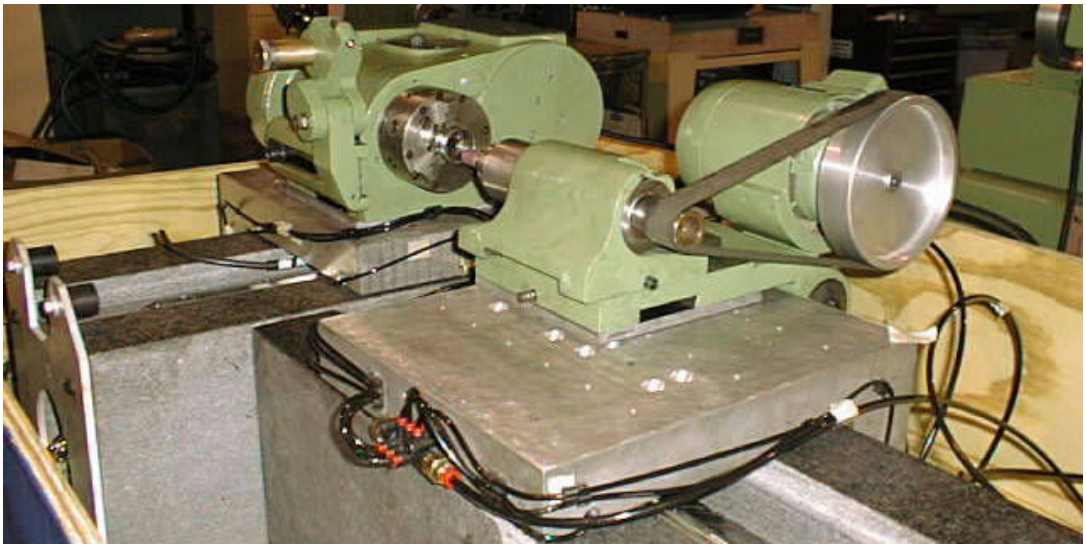

Fig. 14 Bench level prototype system

Fig. 15 Test parts ground on the bench level prototype system. Part: roller bearing inner ring. Material: AISI 52100. Hardness: 57-62 Rc. Maximum stock removal : 0.300 mm on diameter. Required process: Grind the bore diameter and maintain 0.4 Ra or better surface finish and 0.005 mm or less taper and straightness. Incoming part condition: Back face (locating surfac e) and OD were ground.

Lift (μm)	Supply pressure (atm)		Stiffness (N/μm)		Efficiency, η		h_4/h_5	k_4/k_5	ζ_4/ζ_5
load (N)	4	5							
400	18.5	25.0	22	16	0.19	0.15	1.4	1.4	2.5
500	15.5	21.0	33	25	0.25	0.20	1.4	1.3	2.5
600	13.0	17.5	40	29	0.25	0.19	1.3	1.4	2.4
700	11.0	14.5	50	33	0.27	0.19	1.3	1.5	2.3
800	9.0	12.0	50	40	0.22	0.19	1.3	1.3	2.4
900	7.5	10.0	67	50	0.24	0.19	1.3	1.3	2.4
1000	6.3	8.5	80	67	0.24	0.22	1.4	1.2	2.5
1100	5.0	7.0	80	67	0.19	0.18	1.4	1.2	2.7
1200	3.8	5.5	80	67	0.15	0.14	1.5	1.2	3.2

Table 1 Bearing performance data for 50mm x 100 mm commercially available porous graphite air bearing pad derived from Fig. 3 (www.newwaybearings.com)

Freq (Hz)	Damping (%)	Q	Comments
Air on			
362	3.8	26	Twisting
487	1.9	53	Carriage spreading like a “hinge”
607	3.3	30	Center oscillating in z.
Air off			
1430	0.6	167	Top center of carriage oscillating
501	1.3	77	Whole carriage moves up and down in Z.

Table 2 Experimental modal analysis on the Bench Level Experiment system

PART	Roundness @ R1	Roundness @ R2	Roundness @ R3	Ra @R1	Ra @R2	Ra @R3
	µm	µm	µm	µm	µm	µm
1	6.2	6.7	6.6	0.43	0.43	0.62
2	6.1	4.6	5.1	0.47	0.42	0.48
3	11.0	10.1	11.4	0.26	0.31	0.38
4	10.9	10.5	9.5	0.35	0.27	0.27
5	10.9	8.1	7.6	0.51	0.35	0.36
6	8.3	14.9	6.2	0.80	0.49	0.48
7	8.8	7.0	6.4	0.65	0.45	0.43
8	14.2	19.7	17.7	0.73	0.52	0.51
9	18.3	22.3	26.3	0.88	0.52	0.53
10	19.2	22.9	24.5	0.87	0.35	0.43

Table 3 Roundness and surface finish of rough ground test parts: 1) R1 (reading 1) is at the step end, R2 middle, R3 opposite end; 2) roundness measurement conditions: filter 50 cpr, 3 mm stylus, least squares circle evaluation; 3) surface finish measurement conditions: (6) 0.8 mm cut offs, measured on a S-5 form Talysurf with a 0.2 µm tip radius stylus.